THE ASTROPHYSICAL JOURNAL, 350:732–744, 1990 February 20

PULSAR MAGNETOSPHERES WITH JETS

MARTIN E. SULKANEN
Department of Physics, Cornell University, and Space Plasma Physics Group, Los Alamos National Laboratory
AND
RICHARD V. E. LOVELACE
Department of Applied and Engineering Physics and Department of Astronomy, Cornell University
Received 1989 April 17; accepted 1989 August 19

ABSTRACT

We study solutions of the Grad-Shafranov equation which describe ideal magnetohydrodynamic (MHD) flows around a magnetized, rotating neutron star, where the rotation and magnetic axes are identical. The "force-free" limit of this equation is identical to the so-called pulsar equation. We derive the pulsar equation from a variational principle that minimizes the electromagnetic field energy subject to the constraints of fixed total angular momentum and total magnetic helicity. This procedure allows one to apply a result from fusion plasma theory, which suggests a specific form of the magnetic helicity for the configuration. This removes an indeterminancy from the pulsar equation which was not resolved in earlier attempts to find a unique equation for the electromagnetic fields. The pulsar equation is found to be a piecewise linear partial differential equation with a class of solutions that include self-collimated electromagnetic jets along the rotation axis of the star. These jets are confined by magnetic pinching and carry energy, angular momentum, and electric current far away from the star.

We calculate numerically the global field structure for pulsar magnetospheres that contain electromagnetic jets. A principal result is that all of the poloidal magnetic field is confined within the light cylinder of the star, either as closed field loops connected to the surface of the star or as part of the jets. This yields a unique magnetospheric field topology with specific jet characteristics. We discuss the applicability of this model to compact synchrotron nebulae that have been observed in supernova remnants.

Subject headings: hydromagnetics — pulsars — stars: neutron

I. INTRODUCTION

A new class of objects has emerged in the past few years that may indirectly indicate the presence of a pulsar within a supernova remnant—*compact synchrotron nebulae* (CSNs; Kafatos and Henry 1985). The characteristic appearance of these objects is a diffuse cloud of emission with a brightness distribution that is centrally peaked. Approximately 20 of these objects have been detected so far, in wavebands from radio waves to X-rays. A few of these have been observed in more than one region of the spectrum (Weiler 1985). Their flat radio flux spectrum ($S[\nu] \sim \nu^{-\alpha}$, with $\alpha \simeq 0$ for 0.4 GHz $\leq \nu \leq$ 5.0 GHz), the hard, featureless spectrum in the X-rays, and their strong linear polarization (fractional polarizations of 5%–25%) indicate that the synchrotron emission illuminates the nebulae. CSNs have been detected alone, at the centers of supernova remnants, and with known radio pulsars. All the known pulsars within supernova remnants are *also* located within a CSN (however, one pulsar within a remnant is also part of a compact binary system, and its emission overwhelms any observable CSN). The most famous CSN is the Crab Nebula, where synchrotron emission is observed in the radio, optical, and X-ray regions of the spectrum and is so intense that it dominates the emission from a classical supernova shell.

It is clear that the power source for the Crab Nebula is the pulsar 0531+21 located within it. The estimated total luminosity of the nebula is 10^{38} ergs s^{-1}, which is comparable to the measured spin-down energy loss rate $\dot{E} \simeq 5 \times 10^{38}$ ergs s^{-1} of the pulsar. The short lifetime of the high-energy synchrotron-emitting particles requires either replenishment from the pulsar or reacceleration within the nebula. Because the smaller X-ray nebula is located near the pulsar, it is likely that the pulsar provides the high-energy charged particles, which then diffuse outward to form the bulk of the optical and radio nebula. Finally, the relatively strong magnetic field in the nebula (10^{-3} to 10^{-4} G) suggests that the pulsar's magnetic field is wound up within the nebula by its rotation.

Models for CSNs have been developed by Rees and Gunn (1974), and more recently by Kennel and Coroniti (1984). The basic mechanism in both of these models is a strong relativistic MHD wind that emerges from the light cylinder surface of the pulsar, carrying power in both bulk particle flow and magnetic field. Because the expansion velocity of the outer boundary of the nebula is subsonic, the wind undergoes a shock at a distance $R_s \simeq 0.1 R_{neb}$ from the pulsar, where R_{neb} is the radius of the nebula. Beyond R_s, the flow is randomized, and it is there that the bulk of the synchrotron radiation is emitted. This structure would explain the observed underluminous zone around the pulsar (Schmidt, Angel, and Beaver 1979). The relatively large synchrotron surface brightness of the Crab Nebula compared to other CSNs may be explained by the large amount of power that the pulsar supplies and by the relatively small size of the nebula (caused by the anomalously small expansion velocity of the supernova shell).

These models concentrate upon deriving the parameters which describe the wind, namely, the ratio of the Poynting flux to the kinetic energy flux upstream of the shock and the Lorentz factor of the flow upstream of the shock. They assume spherical symmetry and do not attempt to solve for self-consistent fields in the vicinity of the pulsar (i.e., within the light-cylinder).

Many of the synchrotron nebulae, including the Crab Nebula, show considerable elongation. This elongation may be caused by inhomogeneities in the confining interstellar plasma or by inhibited expansion of the supernova remnant transverse to a large-scale interstellar magnetic field. However, it is also possible that *the pulsar's magnetosphere injects momentum and energy along a preferred axis in the form of "jets."*

Beaming from galactic sources exists in compact binary systems. The X-ray binary SS 433 exhibits spectacular beaming with oppositely directed relativistic jets (Margon 1984). Electrodynamic dynamo models involving an accretion disk may power jets often seen in extragalactic radio sources (Lovelace 1976; Blandford 1976; Lovelace, Wang, and Sulkanen 1987, hereafter referred to as LWS). The jets we discuss which may produce the beaming in CSNs require neither a binary system nor an accretion disk; rather, they are part of the structure of the (isolated) pulsar magnetosphere. Benford (1984) considered the behavior of the magnetic field lines near the magnetic poles of a pulsar where the magnetic and rotation axes were nearly aligned. He argued that the plasma flow from the pulsar would be turbulent except near the rotation axis, where the toroidal field is wrapped to produce a current-carrying plasma beam with a radius equal to the "light cylinder radius" of the pulsar; $r_{lc} \equiv c/\Omega_*$, where Ω_* is the angular rotation velocity of the star. This discussion did not attempt self-consistent calculation. Michel (1985) considered the motion of charged test particles in a simple model for the electromagnetic field of a pulsar's wind. He found that in the case where the rotation axis and the magnetic axis were aligned, the particle trajectories were directed toward the rotation axis of the star. This calculation did not consider the back effect of the charged particles' motion on the electromagnetic fields.

In this paper, we describe self-consistent solutions to the near-field region of an aligned rotating and magnetized neutron star. The solutions include electromagnetic jets which can extend to large distances (several light cylinder radii) along the rotation axis of the star. The jets arise from solutions of the "pulsar equation" (Scharlemann and Wagoner 1973), which governs the electromagnetic field structure near the star. The pulsar equation was first described by Scharlemann and Wagoner (1973), Michel (1973*a*), and Cohen, Coppi, and Treves (1973). The radii of the jets is less than r_{lc}, and the jets carry energy, angular momentum, and electric current away from the star. In § II, we derive the "pulsar equation" using a variational principle for the steady state structure of the magnetosphere. *We postulate that the magnetospheric plasma relaxes to an equilibrium subject to fixed angular momentum and magnetic "helicity."* Consequently, we have a strong constraint on the form of the magnetic helicity for the configuration. This removes an indeterminancy from the pulsar equation which has frustrated earlier attempts to find a unique solution for the electromagnetic fields. The pulsar equation is found to be a piecewise linear partial differential equation. In § III, we discuss the jet solutions at large axial distances from the star. In § IV, we describe the numerical methods used to determine the global field structure of the magnetosphere, and in § V we describe the results of numerical calculations for a variety of jet and stellar parameters. We summarize our results and discuss briefly the effect of magnetospheric jets upon models for CSNs in § VI.

II. THE PULSAR EQUATION FROM A VARIATIONAL PRINCIPLE

We review briefly the equations which describe MHD equilibrium around a rotating magnetized neutron star, where its magnetic axis and rotation axis are identical. The derivation here is similar to that given by Scharlemann and Wagoner (1973) for the "pulsar equation," and by Lovelace *et al.* (1986) for the relativistic Grad-Shafranov equation. We assume (i) a steady state, axisymmetric, z-reflection symmetric system, (ii) that the effects of pressure, gravity, and collisions are negligible, and (iii) that the star is uniformly rotating, perfectly conducting, and threaded by all of the magnetic field lines in the configuration (Fig. 1).

The basic equations for the plasma are the mass conservation equation,

$$\nabla \cdot (\rho \boldsymbol{v}) = 0 , \tag{1}$$

where ρ and $\boldsymbol{v}$ are the plasma mass density and flow velocity; the Euler equation

$$\rho_e \boldsymbol{E} + \frac{\boldsymbol{J} \times \boldsymbol{B}}{c} = 0 , \tag{2}$$

where ρ_e is the electric charge density and $\boldsymbol{J}$ is the current density, and where we have ignored the contributions from the plasma inertia; Ampere's law,

$$\nabla \times \boldsymbol{B} = \frac{4\pi}{c} \boldsymbol{J} , \tag{3}$$

with $\nabla \cdot \boldsymbol{J} = 0$; Coulomb's law

$$\nabla \cdot \boldsymbol{E} = 4\pi\rho_e ; \tag{4}$$

Faraday's law

$$\nabla \times \boldsymbol{E} = 0 ; \tag{5}$$

Ohm's law

$$\boldsymbol{E} + \frac{\boldsymbol{v} \times \boldsymbol{B}}{c} = \frac{\boldsymbol{J}}{\sigma} , \tag{6}$$

where σ is the plasma conductivity, here taken to be extremely large so that the right-hand side of equation (6) is arbitrarily small.

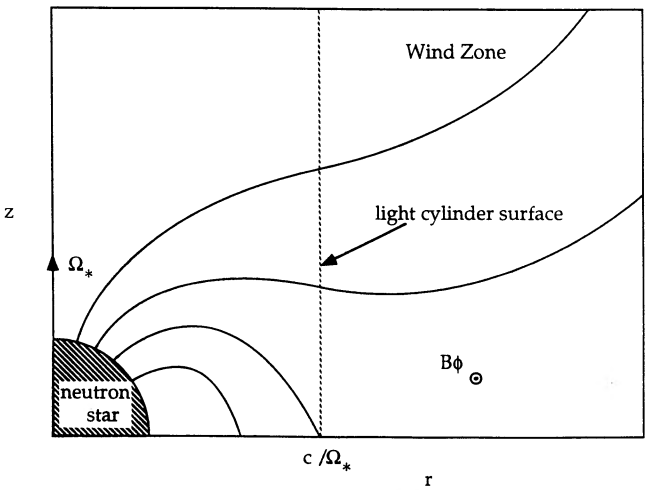

FIG. 1.—Schematic picture of the magnetosphere of an "aligned rotator" pulsar (adapted from Mestel, Phillips, and Wang 1979). Here x and y are the poloidal coordinates scaled by the light cylinder radius. Also shown is the region of the magnetosphere included in the variational volume, defined by a cylindrical can of radius $x = 1$ and $y = Y \gg 1$. The volume excludes a small layer of thickness ϵ along the equator and the surface of the star.

In this axisymmetric system, it is most convenient to describe the poloidal magnetic field in terms of the flux function $\Psi(r, z)$:

$$B_r(r, z) = -\frac{1}{r}\frac{\partial \Psi}{\partial z}, \quad B_z(r, z) = \frac{1}{r}\frac{\partial \Psi}{\partial r}, \tag{7}$$

where $\Psi = rA_\phi$, with A_ϕ the toroidal component of the vector potential. Surfaces of constant Ψ are formed by rotating the poloidal projection of a magnetic field line around the z-axis.

By axisymmetry and equation (5), it follows that $E_\phi = 0$. The poloidal component of the plasma velocity given by equations (5) and (6) is parallel to the poloidal magnetic field; $\boldsymbol{v}_p = \kappa(r, z)\boldsymbol{B}_p$. The mass conservation equation (1) then implies that $\boldsymbol{B}_p \cdot \nabla(\rho\kappa) = 0$. We therefore have that

$$\rho(r, z)\kappa(r, z) \equiv \frac{F(\Psi)}{4\pi}, \tag{8}$$

where F is an arbitrary function of Ψ. It then follows that $\boldsymbol{v} \times \boldsymbol{B} = r^{-1}(v_\phi - \kappa B_\phi)\nabla\Psi$. With this result, we can use Faraday's law and the condition of perfect conductivity to find that

$$\frac{(v_\phi - \kappa B_\phi)}{r} \equiv \Omega(\Psi), \tag{9}$$

and

$$\boldsymbol{E} = -\frac{\Omega(\Psi)}{c}\nabla\Psi, \tag{10}$$

where Ω is another arbitrary function of Ψ. The plasma velocity can then be written as

$$\boldsymbol{v} = \frac{F(\Psi)}{4\pi\rho(r, z)}\boldsymbol{B}_p + \left[\frac{F(\Psi)}{4\pi\rho(r, z)}B_\phi + r\Omega(\Psi)\right]\hat{\boldsymbol{\phi}}. \tag{11}$$

The toroidal component of the Euler equation (2) along with the condition that $E_\phi = 0$ gives

$$\boldsymbol{B}_p \cdot \nabla H(\Psi) = 0, \tag{12}$$

where $H(\Psi) \equiv rB_\phi$ is a third arbitrary function of Ψ. If we write the magnetic field as $\boldsymbol{B} = \nabla\Psi \times \nabla\phi + H(\Psi)\nabla\phi$, where $\nabla\phi \equiv r^{-1}\hat{\boldsymbol{\phi}}$, then the current density can be written as

$$\frac{4\pi}{c}\boldsymbol{J} = H'\boldsymbol{B}_p - \frac{\Delta^*\Psi}{r}\hat{\boldsymbol{\phi}}, \tag{13}$$

where $H' \equiv dH/d\Psi$ and $\Delta^* \equiv \partial^2/\partial r^2 - r^{-1}\partial/\partial r + \partial^2/\partial z^2$. Using this result, along with equations (9) and (10), the component of the Euler equation along $\boldsymbol{B}_p$ is identically zero, while the component parallel to $\nabla\Psi$ gives the "pulsar equation":

$$\left[1 - \frac{(r\Omega)^2}{c^2}\right]\Delta^*\Psi - \frac{1}{2r^2}\nabla\left[\frac{(r^2\Omega)^2}{c^2}\right] \cdot \nabla\Psi + HH' = 0. \tag{14}$$

Because $\boldsymbol{v} \cdot \boldsymbol{E} = 0$ and $\boldsymbol{J} \cdot \boldsymbol{E} = 0$, the bulk Lorentz factor of the plasma is a constant along the field lines; $\gamma \equiv (1 - \boldsymbol{v} \cdot \boldsymbol{v}/c^2)^{-1/2} = \gamma(\Psi)$. The energy conservation equation implied by the ideal MHD equations (1)–(6) is

$$\nabla \cdot \boldsymbol{S}_P = 0, \tag{15}$$

where $\boldsymbol{S}_P$ is the Poynting flux of the electromagnetic field. The poloidal component of $\boldsymbol{S}_P$ is $-\Omega H\boldsymbol{B}_p/4\pi$. Including the plasma bulk kinetic energy in the poloidal energy flux density $\mathcal{S}$ gives $\mathcal{S} = (F[\gamma - 1]c^2 - \Omega H)\boldsymbol{B}_p/4\pi$. We can then see that the condition for the "force-free" assumption is

$$\frac{F(\gamma - 1)c^2}{|\Omega H|} \ll 1. \tag{16}$$

The left-hand side of equation (16) is only a function of Ψ. Thus, if this inequality is satisfied anywhere on a surface of Ψ, then it holds everywhere on this surface.

The pulsar equation is the "force-free" limit of a Grad-Shafranov equation which describes general axisymmetric ideal MHD equilibria (Lovelace *et al.* 1986). One result of this formalism is to identify several presumably arbitrary functions of the poloidal magnetic flux $\Psi(r, z)$ which specify a particular solution of the Grad-Shafranov equation. In the force-free limit considered here, only two of these functions are important. One is identified from Faraday's law and the assumption of perfect conductivity,

$$\Omega(\Psi) \equiv r^{-1}(v_\phi - \kappa B_\phi), \tag{17}$$

where $\Omega(\Psi)$ is identified as the angular velocity of the poloidal field lines. In the pulsar magnetosphere where all the field lines thread the star, $\Omega(\Psi)$ is fixed to be the angular velocity of the star, Ω_*. The other important flux function is derived from the toroidal component of the Euler equation, which implies angular momentum conservation on each flux surface,

$$H(\Psi) = rB_\phi. \tag{18}$$

From this equation and Ampere's law, we can see that a physical interpretation for H is that $2H(\Psi)/c$ is the poloidal current which flows within the flux surface defined by Ψ = constant.

In contrast with $\Omega(\Psi)$, the pulsar equation does not directly imply a particular functional form for $H(\Psi)$. Michel (1982) observed that $H(\Psi)$ is completely arbitrary except that $H(0) = 0$, to avoid a singular current along the z-axis, and that $H = 0$ on the equatorial plane ($z = 0$) because of the even field symmetry $[\Psi(r, z) = +\Psi(r, -z)]$ (where H cannot be simply a function of Ψ). Beyond these restrictions, it has been assumed previously that there are no other physical constraints on the form of H.

Solutions to the pulsar equation have been obtained assuming that H was a simple analytic function of Ψ. The case in which $H \propto \Psi$ leads to a linear equation for Ψ which can then be solved numerically. Michel (1973*a*) considered solutions for Ψ within the light cylinder for $H(\Psi) \equiv 0$ everywhere. Physically, these solutions correspond to a rigidly corotating magnetosphere. Solutions with H = constant are identical to these, with the superposition of singular toroidal magnetic field from a line current along the z-axis. Michel (1973*b*) also considered the case where H is a second-order polynomial in Ψ, which admits solutions where no net axial current flows in the poloidal half-plane (eq. [2]). This choice leads to an analytic solution for Ψ, yielding an monopolar magnetic field. Pellizari (1974) considered H as higher order polynomials of Ψ of the form $H(\Psi) = -(1 - [\Psi/\Psi_c]^n)$, with $\Psi_c \equiv \Psi(r = R_{lc}, z = 0)$ and n an arbitrary integer. Once again, this choice yields closed poloidal current loops in each half-plane of the magnetosphere. Numerical calculations of the resulting $\Psi(r, z)$ were then determined both inside and outside the light-cylinder (*separately*) for various values of $n \geq 0$. Pellizari found that, in general, B_z was discontinuous at the light cylinder surface, requiring a toroidal current sheet there. This discontinuity could be mini-

mized for the choice of H as a linear function of Ψ, $H(\Psi) = H_0 - K\Psi$, but the sheet current could not be removed entirely. Scharlemann and Wagoner (1973) similarly considered a piecewise linear form for H, with H_0 and K as defined above identically zero in a closed corotating magnetosphere, and $H_0 = 0$, $K \neq 0$ in the open field line region. For this selection of H, the pulsar equation is everywhere a (piecewise) linear partial differential equation in Ψ. They solved for the eigenfunctions for the open field line region, assuming that they decreased exponentially with z and that the functions were well behaved through the light cylinder surface. However, they did not attempt to construct a complete solution from these eigenfunctions that would join the open field line regions and the closed magnetosphere consistently.

In summary, the global solutions to date of the aligned rotator magnetosphere are unphysical, and $H(\Psi)$ has been specified without physical basis. A physical basis for H can, however, be found by formulating the equilibrium problem as a *constrained variational principle* (Taylor 1974). As a simple example, consider the equilibria of a force-free plasma with negligible gas pressure (Freidberg 1982):

$$\nabla \times \boldsymbol{B} = \lambda \boldsymbol{B} , \tag{19a}$$

where λ is a function such that

$$\boldsymbol{B} \cdot \nabla \lambda = 0 , \tag{19b}$$

so that $\lambda = \lambda(\Psi)$. The corresponding Grad-Shafranov equation can be written as

$$\Delta^* \Psi + HH' = 0 , \tag{20}$$

with H defined as in equation (2), so that $\lambda = H' = dH/d\Psi$. The arbitrariness of H results from the fact that field-aligned currents given in equation (19a) can have any value. However, current conservation implies that the constant of proportionality λ does not vary on a flux surface.

The equilibrium described in equation (19a) can be determined by minimizing the energy

$$\mathscr{U} = \frac{1}{8\pi} \int_V \boldsymbol{B} \cdot \boldsymbol{B} d^3x , \tag{21}$$

where V is the volume of the plasma. A perfectly conducting plasma will evolve toward equilibrium in such a manner that the total helicity,

$$\mathscr{H} \equiv \int_V \boldsymbol{A} \cdot \boldsymbol{B} d^3x , \tag{22a}$$

remains fixed. This can be generalized to include any arbitrary function of Ψ within the integrand; i.e.,

$$\mathscr{H}_\mu \equiv \int_V \mu(\Psi) \boldsymbol{A} \cdot \boldsymbol{B} d^3x , \tag{22b}$$

will also be a fixed quantity. This is true because helicity is strictly conserved on each flux surface $\Psi(r, z)$. Therefore, the appropriate variational quantity or action for the equilibrium is

$$\mathscr{I} \equiv \frac{1}{8\pi} \int_V \boldsymbol{B} \cdot \boldsymbol{B} d^3x + \int_V \mu(\Psi) \boldsymbol{A} \cdot \boldsymbol{B} d^3x . \tag{23a}$$

Writing the magnetic field in terms of derivatives of Ψ and the poloidal vector potential $\boldsymbol{A}_p$, the action becomes

$$\mathscr{I} = \frac{1}{8\pi} \int_V \left[\frac{(\nabla\Psi) \cdot (\nabla\Psi)}{r^2} + (\nabla \times \boldsymbol{A}_p) \cdot (\nabla \times \boldsymbol{A}_p) + 8\pi\mu(\Psi)\Psi \nabla\phi \cdot (\nabla \times \boldsymbol{A}_p) + 8\pi\mu(\Psi) \nabla\phi \cdot (\boldsymbol{A}_p \times \nabla\Psi) \right] r\, dr\, d\phi\, dz \tag{23b}$$

The Lagrangian L is the integrand in the brackets of equation (23b). The Euler-Lagrange equations for variations in Ψ, A_r, and A_z,

$$\nabla \cdot \left[\frac{\partial L}{\partial(\nabla\Psi)} \right] - \frac{\partial L}{\partial \Psi} = 0 , \tag{24a}$$

and

$$\nabla \cdot \left[\frac{\partial L}{\partial(\nabla A_i)} \right] - \frac{\partial L}{\partial A_i} = 0 , \tag{24b}$$

lead to

$$\Delta^* \Psi - 4\pi r B_\phi \left[2\mu(\Psi) + \Psi \frac{d\mu}{d\Psi} \right] = 0 , \tag{25a}$$

and

$$\Psi \nabla(rB_\phi) + 4\pi \nabla(\Psi^2 \mu) = 0 . \tag{25b}$$

Recalling that $rB_\phi = H(\Psi)$, then substituting the result of equation (25b) into equation (25a) recovers the Grad-Shafranov equation (20), where $H(\Psi)$ can be written as

$$H(\Psi) = -4\pi \left[\Psi \mu(\Psi) + \int_0^\Psi \mu(\tilde{\Psi}) d\tilde{\Psi} \right] . \tag{26}$$

From the analysis above, we see that the function $H(\Psi)$, which appears in the pulsar equation, is related to yet another arbitrary flux function $\mu(\Psi)$, which specifies the helicity on any flux surface Ψ in a perfectly conducting plasma.

Under more realistic conditions, the magnetospheric plasma will be (slightly) resistive, so that both helicity and energy will decay toward the equilibrium state. However, the rates at which these quantities decay will usually be very different. "Selective" decay, whereby the plasma in its approach to equilibrium dissipates a small fraction of its total helicity while losing a substantial amount of energy, has been predicted in the relaxation of a plasma by turbulence-driven cascades (Montgomery, Turner, and Vahala 1978; Montgomery and Turner 1982). Qualitatively, this occurs because the plasma energy cascades from large to small spatial scale fluctuations, where it can be dissipated rapidly, while helicity coalesces (by reconnection) from smaller to larger spatial scales where it dissipates slowly. Numerical simulations (Riyopoulos, Bondeson, and Montgomery 1982) have demonstrated a large monotonic decay of the ratio of total plasma energy to helicity during the relaxation to an equilibrium (minimum energy) state.

This behavior supports the hypothesis first proposed by Taylor (1974, 1975) that small departures from perfect conductivity in the plasma act to destroy helicity conservation on individual flux surfaces, while the total helicity, the integral of $\boldsymbol{A} \cdot \boldsymbol{B}$ over the *total* plasma volume, remains approximately

constant. Therefore $\mu(\Psi)$, introduced in equation (22b), is a *constant*. This implies that $H(\Psi)$ is a *linear* function of Ψ:

$$H(\Psi) = -8\pi\mu\Psi , \tag{27}$$

which leads to a linear force-free equation (19a).

We can apply this result to the pulsar magnetosphere by deriving the pulsar equation from a variational principle. Here we seek an action functional for the pulsar equation which is physically motivated. A mathematical variational quantity for the pulsar equation was discussed briefly by Scharlemann and Wagoner (1973), but its physical basis was not recognized, nor was an attempt made to constrain the form of $H(\Psi)$.

Neglecting inertial terms, the total plasma energy $\mathscr{U}$ is

$$\mathscr{U} = \frac{1}{8\pi}\int_V \boldsymbol{B}\cdot\boldsymbol{B} + \boldsymbol{E}\cdot\boldsymbol{E} d^3x , \tag{28}$$

where the fields are measured in the stationary observer's frame. The inertial terms can be ignored in the energy provided that the $(\gamma - 1)\rho c^2 \ll B^2/8\pi$, or that

$$\gamma \ll |1 - f|\frac{\omega_{c+}}{\Omega_*} , \tag{29}$$

where ω_{c+} is the nonrelativistic cyclotron frequency for the positively charged plasma species (ions or positrons) and f is the relative density of electrons, $f \equiv n_e/n_+$. The values for the ratio ω_{c+}/Ω_* are in excess of 10^4 for ions and 10^7 for positrons, assuming a pulsar period of 1 s and a field strength of $a \approx 10$ G (the stellar field near the light cylinder surface). This ratio scales with Ω_* approximately as Ω_*^2, so that ignoring inertial terms in the total plasma energy is valid for pulsars with short periods ($P < 1$ s).

We take the volume for the variational principle to be a cylindrical can in the upper half volume $z \geq 0$. The can is centered upon the pulsar and extends to the light cylinder surface. The bottom surface of the can avoids the equator and the surface of the star by a small distance ϵ. The axial extent of the cylinder is $L_z \gg r_{lc}$ (Fig. 1).

Goldreich and Julian (1969) estimated the electric field component parallel to the magnetic field for a neutron star in a vacuum. This $E_{\|}$ is typically so large that the magnetosphere will fill with charge drawn off the neutron star. The magnetosphere could also be filled with plasma from magnetospheric pair production (Ruderman and Sutherland 1975) and grain evaporation (Cheng 1985). Violations of the force-free condition (2) are restricted to regions such as a polar "gap" (Ruderman and Sutherland 1975), technically outside of the region of our calculation. We assume also that the conductivity is sufficiently large so that the global helicity constraint of equation (22b) is valid. Thus, $\mu(\Psi)$ is taken to be a constant.

The helicity is a well-defined (i.e., gauge-invariant) quantity when the plasma volume is bounded by magnetic surfaces where $\boldsymbol{B}\cdot d\boldsymbol{S} = 0$, with $d\boldsymbol{S}$ a surface element of the plasma. The surface of the variational volume of Figure 1 does not have this property; however, we can relax this requirement if the steady state condition on the helicity $\mathscr{H}_\mu$ comes from a balance of helicity injection and losses on the boundaries. The helicity flux density can be written as

$$\boldsymbol{Q} = 2\phi_e\boldsymbol{B} - \nabla\times(\phi_e\boldsymbol{A}) , \tag{30}$$

where ϕ_e is the electrostatic potential (Jensen and Chu 1984). We consider the surface integral at the star for a cap centered upon the rotation axis. The outer edge of the cap is defined by the value of Ψ. The surface integral of $\boldsymbol{Q}$ on this cap then gives the rate of helicity injection from the star:

$$\frac{d\mathscr{H}_{in}}{dt} = \iint_{cap}\boldsymbol{Q}\cdot d\boldsymbol{S} = -\left[4\pi\int_0^\Psi \phi_e(\tilde{\Psi})d\tilde{\Psi} - 2\pi\Psi\phi_e(\Psi)\right] . \tag{31}$$

Since the potential ϕ_e is a function only of Ψ, then a similar surface integral for the same field lines that intersect the outer boundaries gives $d\mathscr{H}_{out}/dt = -d\mathscr{H}_{in}/dt$. In principle, helicity transport can occur on all field lines. We will require later that only the field lines that exit from the end caps of the volume in Figure 1 carry helicity.

We consider now any additional constraints that should be imposed upon the equilibrium. The outflow of angular momentum from the rotating star equals that carried by the electromagnetic field through the outer boundary of the can. For an aligned rotator, the constraint of fixed total angular momentum L_z is written as

$$\mathscr{L} = \frac{1}{4\pi c}\int_V \tilde{\Omega}(\Psi)\hat{z}\cdot[\boldsymbol{r}\times(\boldsymbol{E}\times\boldsymbol{B})]d^3x , \tag{32}$$

where $\tilde{\Omega}(\Psi)$ is a flux function with units of angular velocity. As before, the inertial terms are neglected. The boundary condition at the neutron star surface requires that $\tilde{\Omega}(\Psi) \equiv \Omega_*$, the angular velocity of the star. Using equation (6), the final form for the pulsar action, including the constraints of fixed angular momentum and magnetic helicity, is

$$\mathscr{I} = \int_V \left\{\frac{\nabla\Psi\cdot\nabla\Psi}{8\pi r^2}\left[1 - \frac{(\Omega_* r)^2}{c^2}\right] + \frac{(\nabla\times\boldsymbol{A}_p)\cdot(\nabla\times\boldsymbol{A}_p)}{8\pi} + \mu\Psi^2\nabla\phi\cdot[\nabla\times(\Psi^{-1}\boldsymbol{A}_p)]\right\} r\,dr\,dz\,d\phi , \tag{33}$$

which leads to the pulsar equation

$$\left[1 - \left(\frac{r}{r_{lc}}\right)^2\right]\Delta^*\Psi - \frac{2}{r_{lc}}\frac{r}{r_{lc}}\frac{\partial\Psi}{\partial r} + HH' = 0 , \tag{34a}$$

where

$$H(\Psi) \equiv rB_\phi = -8\pi\mu , \tag{34b}$$

with μ a constant.

III. JET SOLUTIONS FOR THE PULSAR MAGNETOSPHERE

We consider now the solutions to the pulsar equation (34a). If we define a dimensionless parameter $\kappa \equiv 4\pi\mu c\Omega_*^{-1} \geq 0$, as well as $x \equiv r/r_{lc}$ and $y \equiv z/r_{lc}$, the pulsar equation can be written as

$$(1 - x^2)\left(\frac{\partial^2\Psi}{\partial x^2} + \frac{\partial^2\Psi}{\partial y^2}\right) - 2x\frac{\partial\Psi}{\partial x} + 4\kappa^2\Psi = 0 , \tag{35}$$

with

$$H(\Psi) = \begin{cases} -2\kappa\Omega_* c^{-1}\Psi, & z > 0; \\ 2\kappa\Omega_* c^{-1}\Psi, & z < 0; \\ 0, & z = 0. \end{cases} \tag{36}$$

Previous studies (§ II; Michel 1973*a*,*b*; Scharlemann and Wagoner 1973) to solve equation (35) have all assumed that the flux function vanishes for large z. We dispense with this assumption and show that field-aligned currents near the z-axis give a solution to equation (34a) which is finite and well

behaved for large z. This requires current flow into the two endcaps located at large $\pm z$ in Figure 1. This charge is replenished by a radial current sheet at the equator, similar to the "pulsar disk" previously discussed by Michel and Dessler (1981). Thus, our solution for the magnetosphere is characterized by large unidirectional poloidal currents in the region where the pulsar equation is valid.

For $z \gg r_{lc}$, we can ignore the z variation in equation (35), so that the pulsar equation becomes

$$(1 - x^2)\frac{d^2\Psi}{dx^2} - \frac{1 + x^2}{x}\frac{d\Psi}{dx} + 4\kappa^2\Psi = 0 . \quad (37)$$

Solutions to equation (37) have been discussed for similar force-free jets proposed to exist in the coronal plasma surrounding the accretion disk of a Schwarzschild black hole (LWS). Briefly, solutions to equation (37) are found to be the hypergeometric series

$$\psi_n = c_n x^2\left[1 + \frac{\alpha\beta}{(1)(2)}x^2 + \frac{\alpha(\alpha + 1)\beta(\beta + 1)}{(2)(2 \times 3)}x^4 + \cdots\right], \quad (38)$$

where c_n is a normalization constant, $\alpha = 1 + \kappa$, and $\beta = 1 - \kappa$. For $x \ll 1$, all solutions behave like $\psi_n \approx x^2$. From this series, we would like to construct a solution to the pulsar equation that is valid for $0 \le x \le X$, where $X \gg 1$. There are, however, physical restrictions on the solutions of equation (37). The field is simply connected to the star, so Ψ must be monotonic in x and must be finite. The series described in equation (38) is finite at $x = 1$ only for $\kappa = 1 + n$, $n = 1, 2, 3, \ldots$. The series terminates after a finite number of terms and then diverges as the highest power of x^2 for large x. The term ψ_n is also an oscillatory function for $x < 1$ for all $\kappa > 1$ (Fig. 2). Clearly the series (38) cannot represent Ψ for all x values at large y.

In order to obtain physical solutions, we reconsider the role of the helicity constraint (i.e., κ) in determining the pulsar equation of § II. We assume that Ψ is given by equation (37) out to the first maximum of ψ_n, designated $\Psi_{jet}(\kappa)$ at $x = x_{jet}(\kappa)$ (Fig. 2). Beyond $x_{jet}(\kappa)$, we take $\Psi = \Psi_{jet}$, which in this region is a solution to equation (37) with $H'(\Psi) = 0$ ($\kappa = 0$). The physical interpretation of this procedure is that only the plasma bounded by the surface $\Psi(r, z) = \Psi_{jet}(\kappa)$ contributes to the helicity in equation (22b). Therefore, μ is *piecewise* constant:

$$\mu = \begin{cases} -\kappa\Omega_*/(4\pi c) , & \Psi \le \Psi_{jet}(\kappa) ; \\ 0 , & \Psi > \Psi_{jet}(\kappa) , \end{cases} \quad (39)$$

and $H(\Psi)$ is a constant for $\Psi > \Psi_{jet}(\kappa)$, given by $-2\kappa c\Psi_{jet}/\Omega_*$ in the upper half-plane. As before, $H(\Psi)$ is discontinuous at the equator. The form for the pulsar equation is then

$$(1 - x^2)\frac{d^2\Psi}{dx^2} - \frac{1 + x^2}{x}\frac{d\Psi}{dx} + 4\kappa^2\Psi\Theta[\Psi_{jet}(\kappa) - \Psi] = 0 , \quad (40)$$

where Θ is the Heaviside step function (with $\Theta[x] = 1$ for $x > 0$ and $\Theta[x] = 0$ for $x < 0$).

Our solution of equation (37) constructed for $z \to \infty$ is a cylindrical jet confined within the light cylinder. The jet is characterized by a magnetic field pitch angle which increases monotonically with x, from 0 at $x = 0$ to $\pi/2$ at $x = x_{jet}$, as shown in Figure 3. The profiles of Ψ, B_z, B_ϕ, E_r, J_z, J_ϕ, and ρ_e for an illustrative case is shown in Figures 4*a* and 4*b*.

Following the results of LWS, we find that the jet carries a poloidal magnetic flux of $\Phi_p = 2\pi\Psi_{jet}(\kappa)$. The jet in the upper half-plane carries a net axial current $I^z_{jet} = -\kappa\Omega_*\Psi_{jet}(\kappa)$. The

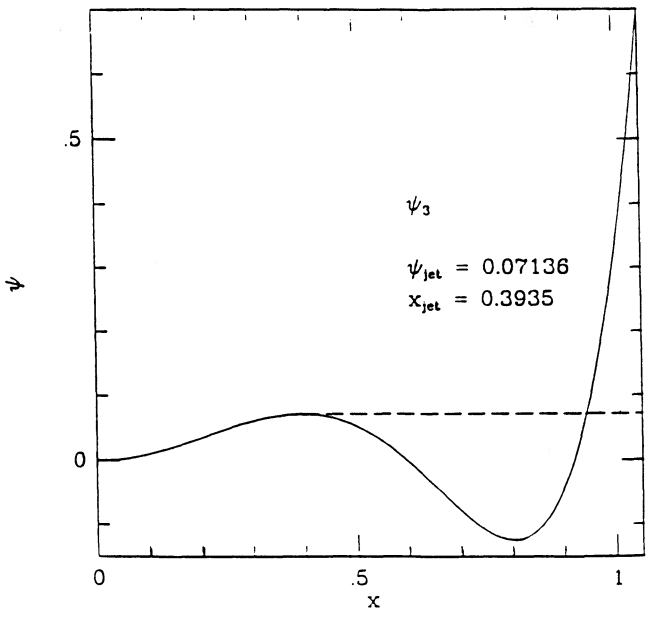

FIG. 2.—Behavior of ψ_3 as given by equation (37) with $c_3 \equiv 1$. Note that all $\psi_n \propto x^2$ for $x \ll 1$. Dashed line indicates the truncation of ψ_3 beyond $x_{jet}(\kappa = 3) = 0.3935$.

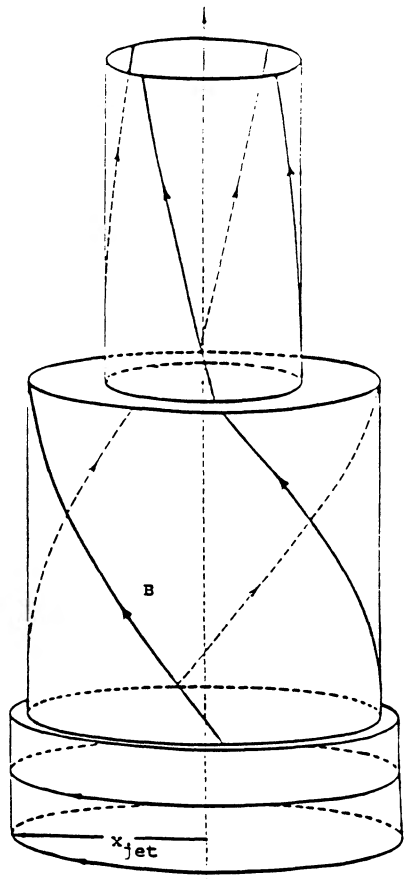

FIG. 3.—Helical structure of the asymptotic pulsar jet for $\kappa = 1.244$

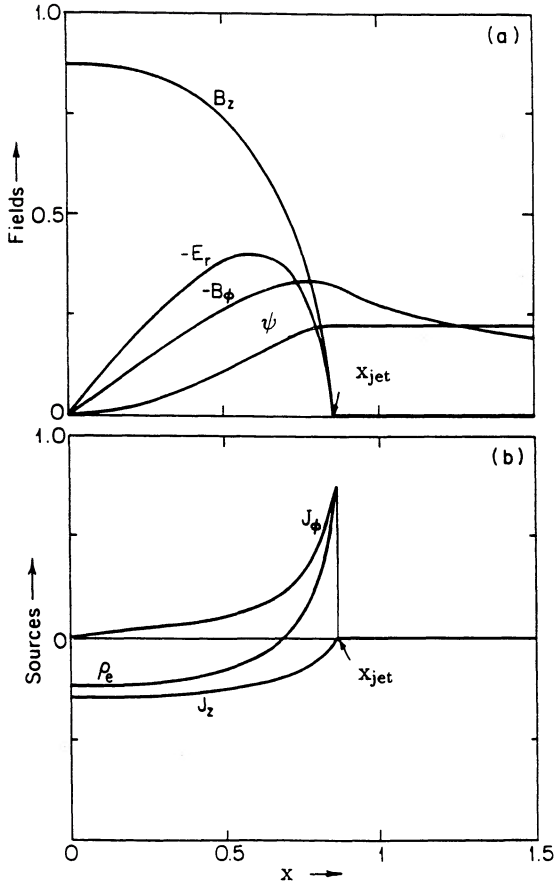

FIG. 4.—Profiles of (*a*) the fields and (*b*) the sources for the pulsar jet with $\kappa = 1.244$. Vertical scale is arbitrary.

current flow in both jets is directed either toward or way from the star. The toroidal current density is given by $dI_\phi/dz = (4\pi)^{-1}cB_z(r = 0)$. There exists also an electric potential drop between the jet radius r_{jet} and the z-axis of $\Delta\phi_e^{jet} = c^{-1}\Omega_* \Psi_{jet}$. The Poynting flux (§ II) gives the total power output from a jet as

$$L_{jet} = \frac{\kappa}{2c}\Omega_*^2 \Psi_{jet}^2 \tag{41}$$

and an angular momentum loss rate of $l_{jet}^z = L_{jet}/\Omega_*$. Finally, the jet's effective impedance is given by $Z_{jet} = 1/(c\kappa)$, so that $Z_{jet} < 30\Omega$.

The electromagnetic sources in the jet are given by

$$\rho_e = -\frac{\Omega_*^3}{4\pi c^3}\frac{1}{x}\frac{d}{dx}\left(x\frac{d\Psi}{dx}\right), \tag{42a}$$

$$J_\phi = -\frac{\Omega_*^3}{4\pi c^2}\frac{1}{x}\frac{d}{dx}\left(\frac{1}{x}\frac{d\Psi}{dx}\right), \tag{42b}$$

$$J_z = \frac{c}{4\pi}H'B_z = -\frac{\Omega_*^3}{2\pi c^2}\kappa\frac{1}{x}\frac{d\Psi}{dx}\ ;\quad \Psi \le \Psi_{jet}\,. \tag{42c}$$

The jet is charge neutral overall ($E_r = 0$ on its surface), but $\rho_e \neq 0$ inside the jet. We note that the poloidal field-aligned currents exist only in the region $\Psi \le \Psi_{jet}$, which is near the polar caps of the neutron star.

The $+z$ jet connects to the northern hemisphere of the star, where plasma effects are assumed to be small and the field is just the intrinsic field of the star. Because the pulsar equation (40) is linear in Ψ, the neutron star's field sets the scale for Ψ and Ψ_{jet}. We define a parameter ζ such that $\Psi_{jet} = \zeta\Psi_*$, where Ψ_* is the maximum flux of the neutron star. (For a dipole stellar field, the maximum flux occurs at the equator and is given by $\Psi_* = \mu_* r_*^{-1}$, where μ_* is the magnetic moment of the neutron star.) Thus ζ measures the fraction of flux emanating from the star that goes into the jet, so $0 \le \zeta \le 1$. The jet's outputs in terms of Ψ_* are $l_{jet}^z = \kappa\zeta\Omega_*\Psi_*$ and $L_{jet} = \kappa\zeta^2(2c)^{-1}(\Omega_*\Psi_*)^2$. For a pulsar, the scales of these quantities are $2 \times 10^{15}\mu_{*30}r_{*10}^{-1}P_1^{-1}$ A and $7 \times 10^{38}\mu_{*30}^2 r_{*10}^{-2}P_1^{-2}$ ergs s^{-1}, respectively, where μ_{*30} is the magnetic moment of the neutron star in units of 10^{30} G cm^3, and r_{*10} is the stellar radius in units of 10 km.

The value of x_{jet} is a monotonically decreasing function of κ, scaling approximately as κ^{-1} for large κ (LWS).

We consider now the global structure of the magnetosphere. In addition to the jet region, two other topologically distinct regions can exist: (i) that where field lines close within the light cylinder, and (ii) that where the field lines penetrate the light-cylinder surface, which we designate as the closed and wind regions, respectively (Fig. 1). In both the wind region and the closed field line region, $H(\Psi) = rB_\phi$ is a constant, given by equation (36), with $\Psi = \Psi_{jet}$. For finite currents and charge densities in the magnetosphere, the term $(1 - x^2)\Delta^*\Psi$ in the pulsar equation vanishes. With $H' = 0$ in these regions, the pulsar equation at $x = 1$ implies that $B_z(r = r_{lc}) = 0$. That is, if field lines penetrate the light cylinder surface, then they do so with their poloidal components normal to the surface.

Because the poloidal current depends upon H', there are no poloidal currents in the wind region. The toroidal current density at $x = 1$ reduces to $J_\phi = c\rho_e$. The wind region also has a Poynting flux that radiates energy across the light cylinder surface. The power from the wind region is given by

$$L_{wind} = \kappa|\Omega_*|c^{-1}\Psi_{jet}(\Psi_e - \Psi_{jet}) \tag{43}$$

(LWS), where Ψ_e is the flux along the equator at the light cylinder radius. This value of flux labels the last field line in the wind region. Similarly, the angular momentum flow in the wind is $l_{jet}^z = \Omega_*^{-1}L_{wind}$. In the closed region, a Poynting flux exists along the poloidal field, directed toward the equator in both hemispheres. The total power into the equatorial disk is

$$L_{eq} = 2\kappa c^{-1}\Omega_*^2\Psi_{jet}(\Psi_* - \Psi_e)\,, \tag{44}$$

where Ψ_* is the value of the flux at the stellar surface along the equator. The angular momentum flux into the disk is $l_{eq}^z = \Omega_*^{-1}L_{eq}$. Angular momentum is transferred from the neutron star into the disk plasma.

We consider now the behavior of Ψ for large distances away from the star and beyond the light cylinder surface. Field lines of the wind region exit the light cylinder but then cannot cross the equator to reconnect to the star. We assume that the field lines become radial for large radial distances, $(x^2 + y^2)^{1/2} \gg 1$, and that the pulsar equation is valid out to some large outer boundary. Beyond this outer boundary, the field lines bend so as to return to the star. Also in this outer region, the current of the jets returns to the equatorial plane, so as to provide a closed current loop for the system. We expand Ψ in the wind region as a power series in $\tilde{r} = (x^2 + y^2)^{1/2}$,

$$\Psi(\tilde{r}, \mu) = \sum_{n=0}^{\infty}\psi_n(\mu)\tilde{r}^n\,, \tag{45}$$

where $\mu \equiv y/\tilde{r}$. The pulsar equation then becomes a set of coupled ordinary differential equations in μ:

$$(1 - \mu^2)\psi_0'' - 2\mu\psi_0' = 0 , \quad (46a)$$

$$(1 - \mu^2)\psi_1'' - 2\mu\psi_1' = 0 , \quad (46b)$$

$$(1 - \mu^2)\psi_j'' - 2\mu\psi_j' + j(j-1)\psi_j = \psi_{j-2}'' + \frac{(j-1)(j-2)}{(1-\mu^2)}\psi_{j-2}; \quad j \geq 2 , \quad (46c)$$

where the prime denotes differentiation with respect to μ. The differential equation for both ψ_0 and ψ_1 is the Legendre equation of order zero and degree zero. The solution, therefore, to $\psi_0(\mu)$ is a linear combination of $P_0(\mu) = 1$ and $Q_0(\mu) = \frac{1}{2}\ln([1+\mu]/[1-\mu])$;

$$\psi_0(\mu) = \psi_{00}\ln\left(\frac{1+\mu}{1-\mu}\right) + \psi_{01} , \quad (47)$$

where ψ_{00} and ψ_{01} are constants. Since the flux is a decreasing function of μ, the value of ψ_{00} is less than zero. This solution has been discussed previously (e.g., Ingraham 1973). The value of ψ_{01} is given by the value of the flux on the equatorial plane, so that $\psi_{01} = \Psi_e$. Determining the value of ψ_{00} is not straightforward. The first term of equation (47) diverges as $\mu \to 1$, and we require that $\psi_{00} < 0$ for Ψ to decrease with μ. However, for any finite value of μ, ψ_0 will be equal to $\Psi_{\rm jet}$ for values of $r \geq 1$. One possible approach is to make $\psi_0 \equiv \Psi_{\rm jet}$ for values of μ larger than some critical value μ_c. This confines the wind field to a fan-shaped region along the equator, with a "dead zone" at higher latitudes. This solution is unattractive for two reasons. First, the value for ψ_{00} is dependent upon the choice of μ_c, which is arbitrary. Second, because Ψ is rapidly varying near μ_c, this will introduce a current sheet on the boundary of the dead zone and the fan. However, physically acceptable solutions exist if we require Ψ to be a *constant* beyond the light cylinder. This corresponds to solutions to the inner zone which have no variation of Ψ along the light cylinder surface. These solutions satisfy the pulsar equation (40) trivially for $r > r_{\rm lc}$.

IV. NUMERICAL SOLUTIONS FOR THE MAGNETOSPHERE

The pulsar equation (34a) is an elliptic partial differential equation with one peculiar feature: along the line $r = r_{\rm lc}$, the term containing the second derivatives vanishes, and equation (34a) becomes a first-order partial differential equation in r. Michel (1973*a*) and Ingraham (1973) have pointed out that the line $r = r_{\rm lc}$ separates the space into two regions which can be solved *independently* for Ψ. Pellazari (1974) used this to solve for Ψ numerically for $H(\Psi) \propto (1 - [\Psi/\Psi_c]^n)$, with $\Psi_c \equiv \Psi_c(r_{\rm lc}, 0)$. The pulsar equation (34a) at $r = r_{\rm lc}$ was used as an effective boundary condition for the solution of the region within the light cylinder. A nonsingular approximation to the pulsar equation (40) for $x = 1 - \Delta$ is an expansion in powers of Δ, which yields two conditions from the terms in Δ^0 and Δ^1:

$$\frac{\partial\Psi}{\partial x} \propto H(\Psi)H'(\Psi) = 0 , \quad (48a)$$

and

$$2\frac{\partial^2\Psi}{\partial x^2} + \frac{\partial^2\Psi}{\partial y^2} = 0 , \quad (48b)$$

respectively. Equation (48a) follows from the arguments made for the jet solutions in the previous section. If we express the condition (48a) using a centered-difference approximation of the derivatives at $x = 1$, then equation (48b) depends solely on values of Ψ *within* the light cylinder. Thus, it is possible to first solve for Ψ within the light-cylinder. The values of Ψ determined along the light cylinder surface can then be used as a boundary condition for the solution outside of the light-cylinder.

We solve the pulsar equation within the light cylinder as follows: the field symmetry $\Psi(x, y) = \Psi(x, -y)$ implies that we need only solve for $y \geq 0$. The boundary condition at $y = 0$ is $\partial\Psi/\partial y = 0$. We also require that $\partial\Psi/\partial y = 0$ at $y = Y \gg 1$. The boundary condition in x, in addition to condition (48a), is that $\Psi(x = 0, y) = 0$. Rather than solving for Ψ, we solve for the flux due to the magnetospheric plasma

$$\Psi_p \equiv \Psi - \Psi_s , \quad (49)$$

where $\Psi_s(x, y)$ is the vacuum flux function of the magnetic field of the *nonrotating* star, which we specify. Thus $\Delta^*\Psi_s = 0$. The maximum axial distance Y is taken to be sufficiently large that Ψ_s is negligible compared with its value at the stellar surface. Terms in equation (40) which involve Ψ_s are brought to the right-hand side of the pulsar equation and treated as sources, except for the step-function term that is proportional to Ψ_p, which is retained as part of the operator on Ψ_p. Thus, the equation which we solve for Ψ_p is

$$(1 - x^2)\frac{d^2\Psi_p}{dx^2} - \frac{1 + x^2}{x}\frac{d\Psi_p}{dx} + 4\kappa^2\Psi_p\Theta[\Psi_{\rm jet}(\kappa) - \Psi_p - \Psi_s] = 2x\frac{d\Psi_s}{dx} - 4\kappa^2\Psi_s\Theta[\Psi_{\rm jet}(\kappa) - \Psi_p - \Psi_s] . \quad (50)$$

For the following calculations, we have taken the stellar flux to be dipolar:

$$\Psi_s = \frac{\mu_*}{r_{\rm lc}}\frac{x^2}{(x^2 + y^2)^{3/2}} , \quad (51)$$

where μ_* is the stellar magnetic moment. The flux at the star's surface along the equator is μ_*/r_*. Because the ratio $r_{\rm lc}/r_*$ is typically large (except for pulsars with millisecond periods), it is convenient in the numerical calculations to scale the total flux by the quantity $\mu_*/r_{\rm lc}$ and to treat the star as a point dipole located at the origin. The plasma flux is given by

$$\Psi_p(x, y) \equiv \eta\frac{\mu_*}{r_{\rm lc}}\frac{\psi_p(x, y)}{\psi_{\rm jet}(\kappa)} , \quad (52)$$

where $\psi_p(x, Y)$ is the jet solution from equation (38) with the normalization constant $c_n = 1$. Similarly, $\psi_{\rm jet}(\kappa)$ is the dimensionless jet flux with this same normalization. Therefore the physical jet flux is defined to be $\Psi_{\rm jet} = \eta\mu_*/r_{\rm lc}$. The relation between η and ζ, defined in § III, is then $\zeta = (r_*/r_{\rm lc})\eta$. The value of dimensionless magnetic field for ψ near the y-axis is 2, so that the physical magnetic field for the jet there is $B_z = 2\eta\mu_*/r_{\rm lc}^3$. For a 1 s period pulsar, the jet axial magnetic field is approximately η G.

The solution for the magnetosphere is specified by the two parameters κ and η. The total dimensionless flux is given by

$$\psi(x, y) = \psi_p(x, y) + \frac{\psi_{\rm jet}(\kappa)}{\eta}\frac{x^2}{(x^2 + y^2)^{3/2}} . \quad (53)$$

If we fix the value of η and vary the value of κ, we are fixing the fraction of the total stellar flux which the jet contains while

varying the poloidal current that the jet carries. In practice, it is easier to fix κ and to vary the strength of the stellar field by varying η.

We solve for ψ_p within the light cylinder by a finite-difference approximation to equation (50) on a poloidal grid, where the grid points for x are evenly spaced for $x \in [0, 1]$. We anticipate that the behavior of the solutions in y will vary only slowly beyond $y = 1$. Therefore, we transform to a compressed axial variable λ, defined by

$$\lambda \equiv 1 - e^{-y/y_0}, \tag{54}$$

where y_0 is an adjustable scale factor. The maximum value of λ is then $\Lambda = 1 - e^{-Y/y_0} \leq 1$. Finally, we have smoothed the step function in equation (39) so as to improve convergence of the solutions. H' is taken to vary smoothly between 0 and $-2r_{lc}\kappa$ with a width $\sigma\psi_{jet}(\kappa)$, with $\sigma \ll 1$.

V. DISCUSSION OF NUMERICAL SOLUTIONS

Figure 5*a* illustrates a typical numerical solution of the magnetosphere within the light-cylinder. Notice (i) that there is a well-defined jet field along the rotation axis, (ii) that in the wind zone, field lines cross the light cylinder surface normally, and (iii) that there is a region of closed field lines. The closed field line region and wind region are separated by a "y-point" cusp at $x = 1$, $y = 0$. Figure 5*b* shows the contribution of the dipole flux of the star to this solution. The rotation of the star causes less poloidal flux to be enclosed within the light cylinder of the star. In the example of Figures 5*a* and 5*b* the ratio of the total flux to the dipole flux at $x = 1$, $y = 0$ is 1.785. Figure 6 shows the $z \gg r_{lc}$ behavior of ψ, and Figures 7*a* and 7*b* show the fields and sources for the asymptotic jet.

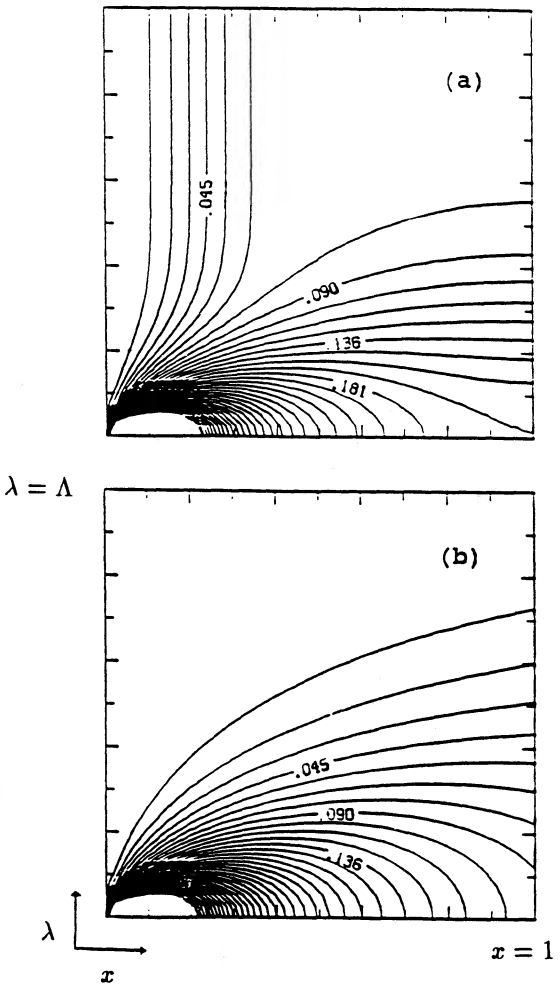

FIG. 5.—Poloidal field line projections, within the light cylinder, for a numerical solution to the pulsar equation (50), with $\kappa = 3$ and $\eta = 1$. The plot here is the compressed (x, λ) coordinate system, with $Y = 4.5$. Contours are of total dimensionless flux, with $\psi(1, Y) = 0.076$. (*b*) Contribution to ψ in (*a*) given by the dipole flux of the star.

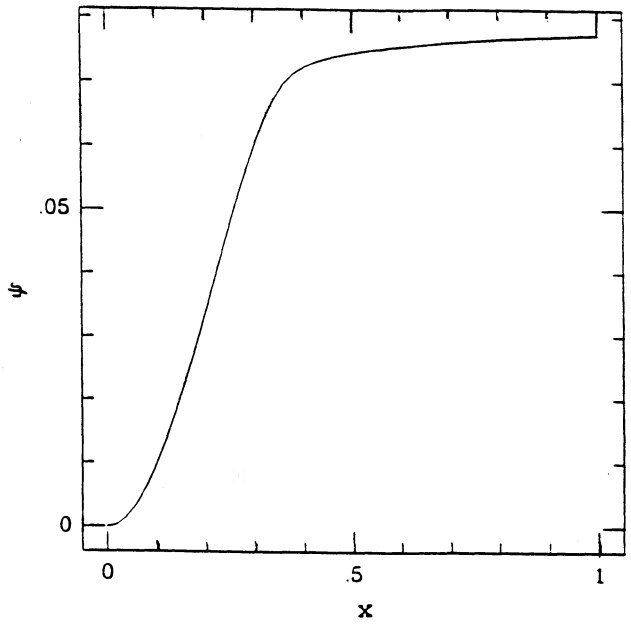

FIG. 6.—Profile of the flux for the jet $\psi(x, Y)$ of Fig. 5. The effect of the smooth rolloff to approximate the step-function in the pulsar equation (50) is to extend the jet to $x = 1$, but with very little variation from the original jet radius $x_{jet}(\kappa = 3) = 0.3935$.

In the magnetosphere solutions we consider, all the jet field lines must originate from the star. The region of (κ, η) parameter space in which there are physical solutions is explored by fixing κ and varying η. That is, we fix the values of the physical jet flux and its current, and we determine the values of the stellar parameter μ_*/r_{lc} which gives physical solutions. Figure 8 shows the variation of the solution with η for $\kappa = 3$. The width of the rolloff $\sigma = 0.001$. We can clearly see that smaller stellar fields (larger η) do not give jet solutions.

One limit in which there are no jet solutions is that where the jet flux is larger than the stellar flux at the equator. We would then see the jet disconnect near the origin. However, the jet disconnects in a region well out into the magnetosphere. Evidently the lack of a jet solution occurs first when there are insufficient magnetospheric currents near the light cylinder surface to support the jet.

Figure 9 shows the region in the (κ, η) parameter space which support jets. The numerically determined maximum allowed values of η for a given κ are also dependent upon the width of the rolloff σ. We have attempted to minimize this dependence by maximizing the grid resolution and choosing the smallest value of σ for which we can find convergent solutions. We identify the value of η where the contour $\psi(x, y) = \psi_{jet}$ first fails to return to the star as the maximum allowed value of $\eta \equiv \eta_{max}$. The numerical uncertainty of η_{max} is approx-

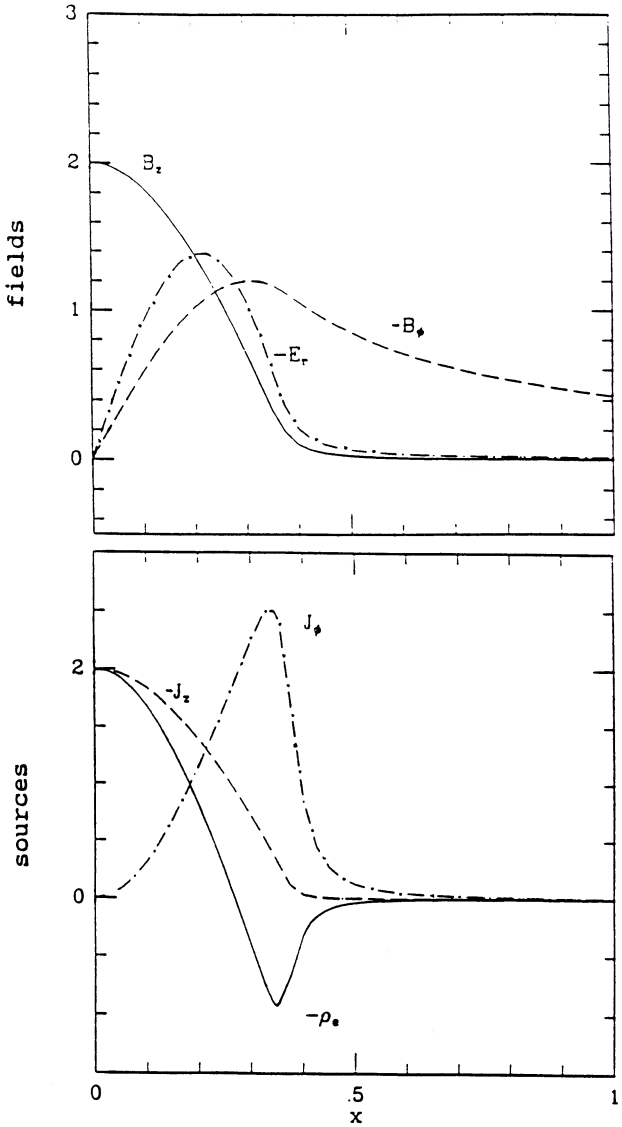

FIG. 7.—Numerical values for the fields (*upper panel*) and sources (*lower panel*) of the asymptotic jet of Fig. 5.

imately ± 0.25. The lower endpoint of Figure 9 is at $\kappa = 1$, below which jets are not possible. The upper κ endpoint is uncertain. We have found that for an (x, y) mesh of 80×77 with $\sigma = 5 \times 10^{-4}$ that convergent jet solutions are no longer possible for $\kappa > 10$, but this may be caused by resolution limits of the grid. It may be that the (κ, η) boundary extends to $\eta \to 0$ as $\kappa \to \infty$.

Figure 10 shows the variation of ψ with λ along the light cylinder surface. The wind zone field lines which traverse the light cylinder surface are confined to a relatively small region above the equator. For all values of η such that the stellar flux is still an insignificant contribution to the asymptotic jet, the total flux along the light cylinder surface becomes constant within $z \simeq r_{lc}$ of the equator. Such "pinching" of the poloidal field has also been seen by Michel (1973*a*) for the case where $H(\Psi)$ is constant within the light cylinder.

Figure 11 shows a typical result for the wind zone field lines in the (x, y) plane. Near the equatorial plane, the field shows a slight divergence with increasing x, consistent with a radial field. However, at higher latitudes the poloidal field becomes nearly parallel to the light cylinder surface; near the surface, the field becomes tightly bunched, suggesting a toroidal current sheet there. The cause of this behavior is the pinching of the field within the light cylinder toward the equatorial plane. All solutions to the inner zone in which poloidal field lines penetrate the light cylinder surface produce such singular solutions in the wind zone.

One solution to the wind zone fields exists which does not exhibit singular behavior, namely that ψ is a constant in the wind zone, so that Ψ_{jet} is identical to Ψ_e. Here all of the poloidal field is confined within the light cylinder, either as part of the jet or of the closed magnetosphere. Because the jets carry current, there is a toroidal field beyond the light cylinder surface, given by $B_\phi = -2\kappa\eta\mu_*/(rr_{lc}^2)$ in the upper half-space, and $B_\phi = 2\kappa\eta\mu_*/(rr_{lc}^2)$ in the lower half-space. A radial current flow in the equatorial plane is, of course, required (§ III).

The solutions for the magnetosphere with jets but no poloidal wind field occur for only one value of κ for a given η. This relation is shown by the curve in Figure 9. These solutions are simpler than those which include a wind zone. The parameter κ, which was previously arbitrary, is now fixed by the fraction of stellar flux carried by the jet. Furthermore, the properties of the jet are uniquely specified. From Figure 9, we see that the maximum value of $\eta \simeq 4$ with $\kappa \simeq 3$, and that $\kappa \simeq 12\eta^{-1}$ for $\eta \gtrsim 4$. Using $r_{*10} = 1$ and $\mu_{*30} = 1$, we have $\zeta \lesssim 2.1 \times 10^{-4}\eta P_1^{-1}$, so that only a small fraction of the star's flux is typically contained in the jet. However, for very short period pulsars (e.g., PSR 1987A), the requirement that $\zeta \leq 1$ may determine the maximum allowed value of η in terms of r_*, μ_*, and P. The last "open" field line at the polar cap, that is, the last field line that is part of the jet, is within an angle $\sin\theta_c = (\eta r_*/r_{lc})^{1/2}$ of the rotation axis. It then follows that $I_{jet}^z \simeq 5.3 \times 10^{12} P_1^{-2}$ A and $L_{jet} \simeq 3.5 \times 10^{32}\eta P_1^{-4}$ ergs s^{-1}. Because for small η, $\kappa \propto \eta^{-1}$, all the possible jets carry the same current, but the maximum jet luminosities occur for the largest values of η. These are jets which carry the maximum fraction of stellar flux. From the numerically determined maximum of $\eta \simeq 4$, the jets contain approximately $1.7 \times 10^{-3} P_1^{-1}$ of the stellar flux, have a radius of $0.4r_{lc}$, and carry a total power of $\dot{E}_{jets} = 2.8 \times 10^{33}\mu_{*30}^2 P_1^{-4}$ ergs s^{-1}. The dependences of $\dot{E}$ here are the same as that for the simple magnetic dipole radiation slowdown for the pulsar (Pacini 1967). Finally, we note that the jet fields are well established within a distance $\approx 2r_{lc}$ along the axis from the pulsar. We therefore suggest that small misalignments ($\theta \ll 30°$) of the magnetic and rotation axes will not substantially alter the structure of the asymptotic jet fields, but will only add small-amplitude modulating fields to the DC magnetospheric fields determined here.

VI. CONCLUSIONS

The pulsar equation, as derived from the ideal MHD equations, is indeterminate. We rederive the pulsar equation from a variational principle in order to emphasize the relation of the flux function $H(\Psi) = rB_\phi$ to the magnetic helicity of the system. Small departures from perfect conductivity suggest (Taylor 1974, 1975) that magnetic helicity is not invariant on an individual flux surface, and that $H(\Psi)$ is specified as a linear function of Ψ (or a constant). This specifies the pulsar equation uniquely as a linear partial differential equation.

Analysis of the pulsar equation for large axial distances from the star reveals solutions which correspond to cylindrical jets.

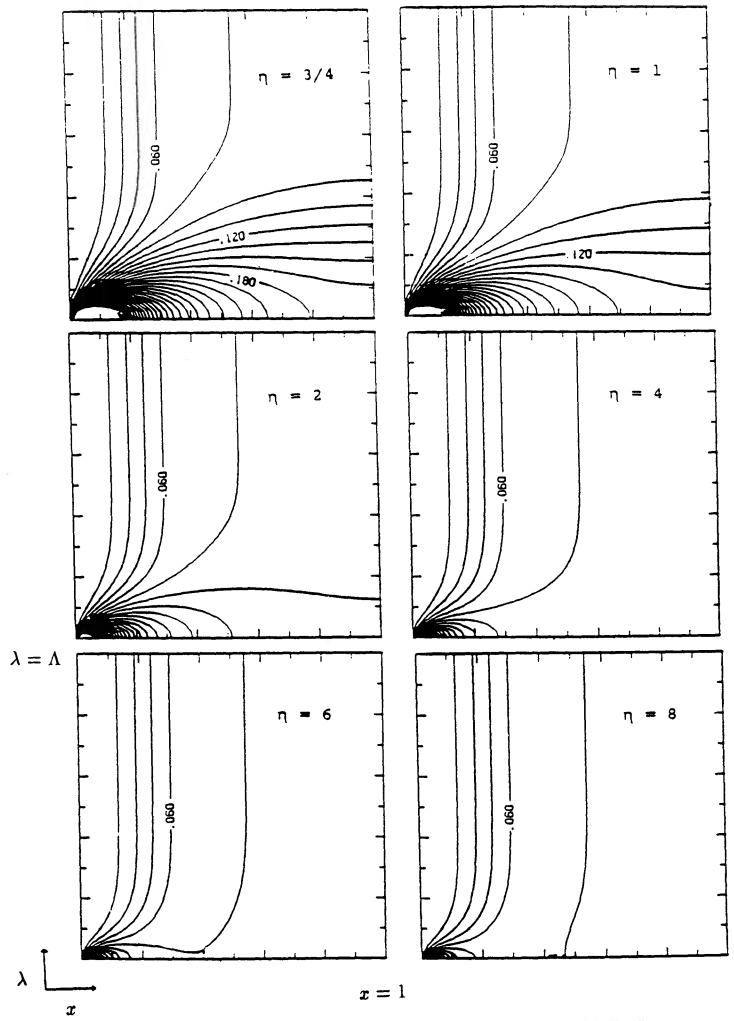

FIG. 8.—Variation with η of the solution described in Fig. 5. The jet disconnects when the stellar field is weak.

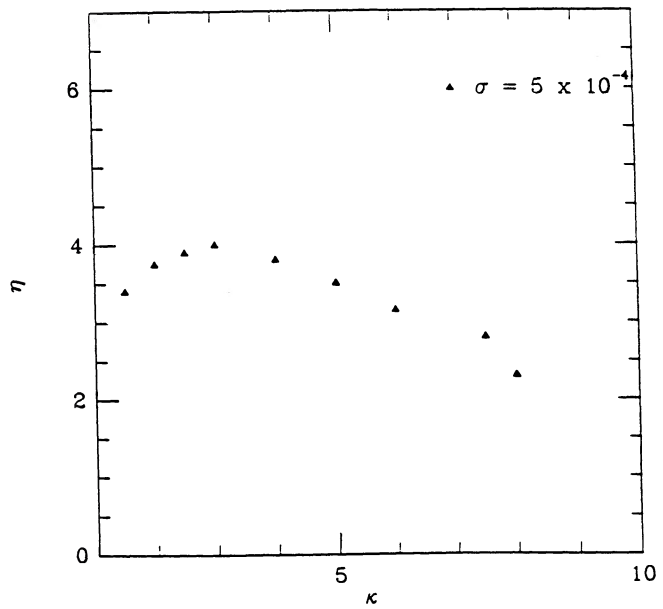

FIG. 9.—The region of (κ, η) parameter space where physical jets exist. Physical jets exist below the curve given by the triangles, where the rolloff parameter $\sigma = 5 \times 10^{-4}$.

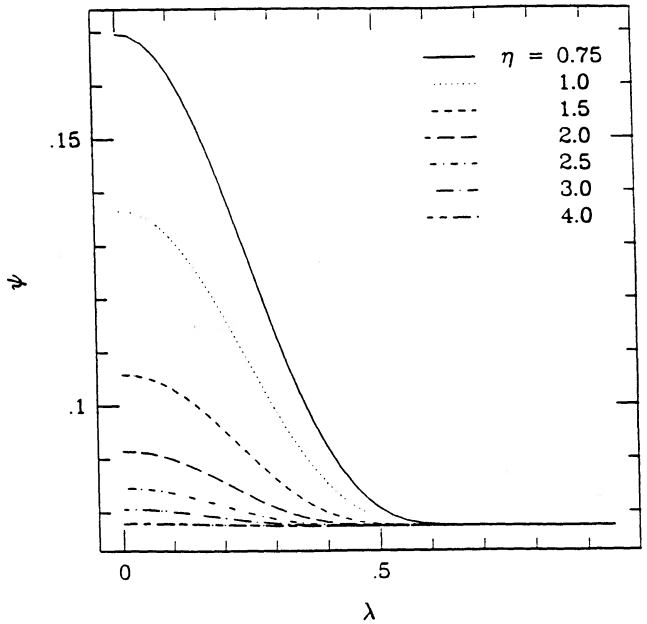

FIG. 10.—Variation of ψ with the compressed dimensionless axial coordinate λ for various values of η. Note that $\lambda = 0.5$ corresponds to $z = 1.04 r_{1c}$.

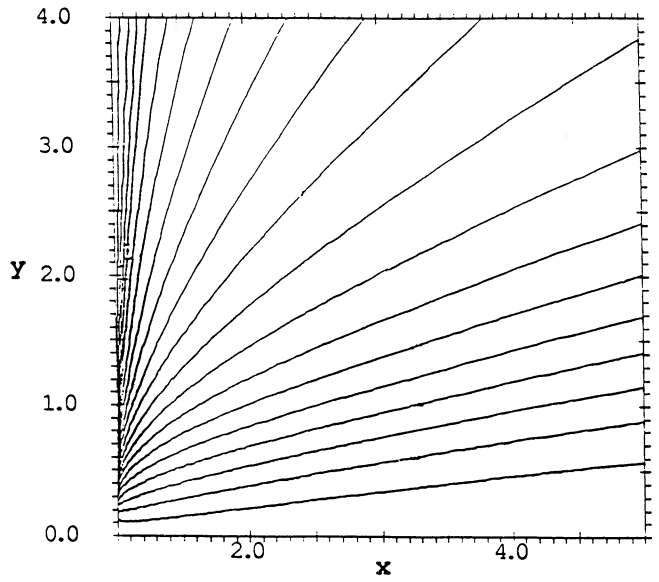

FIG. 11.—Poloidal field lines in the wind zone for $\kappa = 4$ and $\eta = 0.75$. Contour lines are equally spaced between ψ_{jet} and ψ_e. Tightly bunched lines along the light cylinder surface for higher values of y imply a toroidal current sheet.

The jets are collimated within the light cylinder of the star by magnetic pinching and carry energy, angular momentum, and electric current away from the star. Consistent jet solutions are found for the case where the flux function $H(\Psi)$ is proportional to Ψ within the jet and constant outside of the jet. Our interpretation of this is that poloidal (field-aligned) currents are emitted from the star on a fraction of the stellar surface near the rotation axis (the polar caps of the pulsar). The boundary of this region is where $\Psi_*(r, z) = \Psi_{jet}$, where Ψ_* is the flux at the surface of the star.

Numerical solutions to the pulsar equation within the light cylinder indicate that the jets require a minimum stellar magnetic moment to provide the magnetospheric currents to support the jet. That is, jet solutions for a given κ are not possible when η rises above a particular value (Fig. 9). Smaller values of η give solutions which have magnetic field traversing the light cylinder surface, while values of (κ, η) along the curve in Figure 9 give solutions in which the poloidal field vanishes along the light cylinder surface.

The magnetosphere beyond the light-cylinder surface, the wind zone, has been obtained numerically by using the values of the flux function along the light cylinder surface (determined from the interior solution). The solutions which have magnetic field lines penetrating the light cylinder surface are not well behaved in the wind region. We conclude that solutions to the magnetosphere which contain jets have Ψ = constant beyond the light cylinder surface. In these solutions, magnetic field lines from the star are either part of a jet or part of the closed magnetosphere within the light cylinder. Thus, the electromagnetic Poynting flux from the star is carried in oppositely directed beams beamed along the rotation axis.

Finally, we discuss the role of pulsar jets in the formation and structure of compact synchrotron nebulae. Although the jets are charge neutral overall, their local charge density is nonzero. However, on distance scales $L \gg r_{lc}$, we expect the jet to relax to a configuration in which $\boldsymbol{E} \equiv 0$ everywhere in the jet. The time scale for current neutralization, however, is expected to be much larger than that for charge neutralization (Miller 1982). Such a relaxation will conserve the total mass, energy, linear momentum, angular momentum, magnetic flux, and current that is transported by the jet. For the neutralized jet, a large fraction of the spin-down power may be in the form of bulk kinetic energy. The description of the charge-neutral jet equilibrium would require the relativistic Grad-Shafranov equation, which includes the effects of plasma inertia (Lovelace *et al.* 1986). The theory of non–force-free, ideal MHD jets have been developed, but only in the nonrelativistic limit (Blandford and Payne 1982; Mobarry 1988; Koupelis 1988; Lovelace, Mobarry, and Contopolous 1989).

Many of the CSNs exhibit significant elongation; for example, 3C 58, CTB 87, G5.3–1.0, and the Crab Nebula (Kafatos and Henry 1985). The morphology of the sources CTB 80 and G5.3–1.0 suggests large-scale (parsec) jets may be involved. Models of Crab-like remnants (Kennel and Coroniti 1984; Rees and Gunn 1974) have assumed a *spherically symmetric* MHD wind beyond the light cylinder radius of the pulsar that flows toward the nebula. The validity of this assumption depends upon the structure of the self-consistent fields determined within the light cylinder of the pulsar (the source region of the Kennel-Coroniti MHD wind), of which a complete description includes a electron-positron plasma formed by pair production near the stellar surface. Equation (29) suggests that for even a "massive" electron-positron magnetosphere (i.e., a quasi-neutral electron-positron plasma with a net charge density equal to that consistent with the corotation electric field) the "force-free" condition can still be valid within the magnetosphere. Thus, the jet solutions for the magnetospheric fields described in this paper may be a more realistic description of the conditions near the inner boundary of the MHD wind region in the models of Crab-like remnants. As described above, the jets may become charge neutralized, so that the wind is dominated by plasma rather than the original emergent jet electromagnetic fields. Nevertheless, the magnetospheric jets can provide a source for the MHD wind which injects energy, angular momentum, and plasma preferentially along the pulsar rotation axis. The may lead to solutions for the structure of the MHD wind region in CSN models which slow a substantial elongation along the rotation axis.

The authors would like to thank John Wang, Clark Mobarry, and Courosh Mehanian for useful discussions, Meers Oppenheim for an independent numerical confirmation of the wind zone solutions, and Galen Gisler for a critical reading of the manuscript.

REFERENCES

Benford, G. 1984, *Ap. J.*, **282**, 154.
Blandford, R. D. 1976, *M.N.R.A.S.*, **176**, 465.
Blandford, R. D., and Payne, D. G. 1982, *M.N.R.A.S.*, **199**, 883.
Cheng, A. F. 1985, *Ap. J.*, **299**, 917.
Cohen, R. H., Coppi, B., and Treves, A. 1973, *Ap. J.*, **179**, 269.
Freidberg, J. P. 1982, *Rev. Mod. Phys.*, **54**, 801.
Goldreich, P., and Julian, W. H. 1969, *Ap. J.*, **157**, 869.
Ingraham, R. L. 1973, *Ap. J.*, **186**, 625.
Jensen, T. H., and Chu, M. S. 1984, *Phys. Fluids*, **27**, 2881.
Kafatos, M. C., and Henry, R. B. C., ed. 1985, *The Crab Nebula and Related Supernova Remnants* (New York: Cambridge University Press).
Kennel, C. F., and Coroniti, F. V. 1984, *Ap. J.*, **283**, 694.
Koupelis, T. 1988, Ph.D. thesis, University of Rochester.
Lovelace, R. V. E. 1976, *Nature*, **262**, 649.

Lovelace, R. V. E., Mehanian, C., Mobarry, C. M., and Sulkanen, M. E. 1986, *Ap. J. Suppl.*, **62**, 1.
Lovelace, R. V. E., Mobarry, C. M., and Contopolous, J. 1989, in *Proc. Noto Italy Conf. on Accretion Disks and Magnetic Fields in Astrophysics*, ed. G. Belvedere (Dordrecht: Kluwer-Nijhoff), p. 79.
Lovelace, R. V. E., Wang, J. C. L., and Sulkanen, M. E. 1987, *Ap. J.*, **315**, 504 (LWS).
Margon, B. 1984, *Ann. Rev. Astr. Ap.*, **22**, 507.
Mestel, L., Phillips, P., and Wang, Y. M. 1979, *M.N.R.A.S.*, **188**, 385.
Michel, F. C. 1973*a*, *Ap. J.*, **180**, 207.
———. 1973*b*, *Ap. J. (Letters)*, **180**, L133.
———. 1982, *Rev. Mod. Phys.*, **54**, 1.
———. 1985, in *The Crab Nebula and Related Supernova Remnants*, ed. M. C. Kafatos and R. B. C. Henry (New York: Cambridge), p. 55.
Michel, F. C., and Dessler, A. J. 1981, *Ap. J.*, **251**, 654.
Miller, R. B. 1982, *Physics of Intense Charged Particle Beams* (New York: Plenum).
Mobarry, C. M. 1988, Ph.D. thesis, Cornell University.
Montgomery, D., and Turner, L. 1982, *Phys. Fluids*, **25**, 345.
Montgomery, D., Turner, L., and Vahala, G. 1978, *Phys. Fluids*, **21**, 757.
Pacini, F. 1967, *Nature*, **216**, 567.
Pellizari, M. A. 1974, M.S. thesis, Rice University.
Rees, M. J., and Gunn, J. E. 1974, *M.N.R.A.S.*, **167**, 1.
Riyopolous, S., Bondeson, A., and Montgomery, D. 1982, *Phys. Fluids*, **25**, 107.
Ruderman, M. A., and Sutherland, P. G. 1975, *Ap. J.*, **196**, 51.
Scharlemann, E. T., and Wagoner, R. V. 1973, *Ap. J.*, **182**, 951.
Schmidt, G. D., Angel, J. R. P., and Beaver, E. A. 1979, *Ap. J.*, **227**, 106.
Taylor, J. B. 1974, in *Plasma Physics and Controlled Nuclear Fusion, Proc. 5th Internat. Conf., Tokyo* (Vienna: IAEA), p. 161.
———. 1975, *Phys. Rev. Letters*, **33**, 1139.
Weiler, K. W. 1985, in *The Crab Nebula and Related Supernova Remnants*, ed. M. C. Kafatos and R. B. C. Henry (New York: Cambridge), p. 265.

MARTIN E. SULKANEN: ESS-8, Mail Stop D438, Los Alamos National Laboratory, Los Alamos, NM 87545

RICHARD V. E. LOVELACE: Department of Applied and Engineering Physics, Cornell University, Ithaca, NY 14853